

EVLA Memo # 136

EVLA Measurements Close to the Sun: Elevated System Temperatures

Catherine A. Whiting and Steven R. Spangler

Department of Physics and Astronomy

The University of Iowa

Iowa City, Iowa 52242, USA

(Dated: July 28, 2009)

Abstract

This document describes system temperature (T_{sys}) measurements near the sun at 5 GHz with EVLA antennas. The purpose of the test measurements was to measure the solar contribution to the system temperature as a function of angular distance from the sun. At a given angular separation from the sun, the antennas showed a range of system temperatures. The reason for this range is unclear. We based our results on the median T_{sys} of 10 antennas which provided adequate data. There are three significant regions of interest: at $2-3R_{\odot}$ (32-48') the system temperature varies from 100-350 K; at $3-5R_{\odot}$ (48-80') the system temperature is 50-100 K; for separations greater than $5R_{\odot}$ (80') the system temperature levels off to the cold-sky EVLA T_{sys} value of 39 K. A model calculation of the system temperature due to the quiet sun in the sidelobes adequately reproduced the measured T_{sys} values.

I. INTRODUCTION

This document will describe test measurements made to determine the solar contribution to the system temperature as a function of solar offset. Observing near the sun can result in elevated system temperatures. Despite the loss in sensitivity due to this effect, there are many solar coronal phenomena that are interesting to measure. The motivation for these solar offset system temperature measurements is to plan for future solar coronal Faraday rotation observations. An example of such observations is described in Ingleby et al (2007). The observations of Ingleby et al were made at 1.46 and 1.66 GHz and, due to system temperature constraints, were limited to a closest angular distance of $5R_{\odot}$ ($80'$). For our future observations we wish to observe closer to the sun, so we are switching to 5 GHz and are primarily interested in the performance of the EVLA from $2-5R_{\odot}$ ($32-80'$). The results of these test measurements may also be of interest to future observers making observations in the vicinity of the sun. This memo serves to provide that information.

The system temperature is the sum of the receiver temperature and the antenna temperature. The antenna temperature is determined by the antenna beam power pattern, which changes with observing frequency, and the angular separation of the beam center from the center of the sun. Since the antennas were not pointing directly at the sun throughout the observations, the side lobes were the main contribution to the system temperature. A theoretical model for the expected system temperature as a function of solar elongation will be discussed and describes the contribution of the sun in the side lobes.

II. TEST MEASUREMENTS

The observations were made on April 26, 2009 with 20 EVLA antennas. There were two IFs at 4885 MHz (IF 1) and 4835 MHz (IF 2) with right and left polarizations for each IF. Six antennas were edited out at the start due to lost data and an azimuth gearbox failure. The holography mode raster scan was chosen for the observing mode because of its ability to make measurements along a line segment with arbitrary starting point, length, and position angle with respect to the center of the sun. There were three scans starting at about 2 solar radii ($32'$) from the center of the sun. Throughout this document we will quote the solar offsets in units of both solar radii (which is relevant for planning coronal observations) and

arcminutes. The solar radius value we used in quoting the offsets is the mean photospheric radius. The conversion between solar radius and angular interval is

$$1R_{\odot} = 16' \text{ (arcminutes)} \quad (1)$$

The actual photospheric radius on the day of observations was $15'.9$.

The first scan was done at a position angle of 0° , labeled “Horizontal Scan”. A position angle of 0° in the holography mode raster scan means to step in increasing azimuth with constant elevation. The second scan was at a position angle of 45° , labeled “Diagonal Scan”, meaning equal steps in increasing elevation and azimuth at an angle of 45° with respect to the horizon, and the last scan was at a position angle of 90° , labeled “Vertical Scan”, meaning steps in increasing elevation with azimuth constant. The elevation angle of the observations ranged from 63.5° - 69.3° . The antenna beam shape is not azimuthally symmetric (Perley and Hayward 2005) due to the quadrupod legs, so we chose the three different scans to check for possible effects of this on the system temperature. Each pointing was spaced by $0.18R_{\odot}$ ($2.9'$) and there were 38 pointings per scan, ending at $8.9R_{\odot}$ ($142'$). The horizontal scan was shortened (perhaps due to increased slew time of the antennas), and only had 26 pointings, extending out to $6.6R_{\odot}$ ($106'$).

The data were returned in the form of T_{sys} vs time in each of the two polarizations and two IFs. The desired observational function was $T_{sys}(r)$, where r is the angular offset from the sun, given in either solar radii or arcminutes. To obtain the antenna position in relation to the sun, we used the observe file and the time of each pointing and calculated the commanded position of the antennas. We do not have confirmation that the antennas were pointing at the commanded positions for the following reason. In the holography mode that we used it is necessary to have a reference antenna pointing at the center of the sun throughout the observations. This is because the holography mode only recognizes fixed antenna - moving antenna pairs and ignores pairs in which both antennas were moving. This is specific to the holography mode and we did not anticipate the need for this, so we did not use a reference antenna during the observations. We have no reason to believe that the commanded positions were in error. Section III.B. discusses a model which matches the data, indicating that our conversion of the antenna positions is correct.

III. RESULTS

A. Measured Results

The system temperature data were retrieved with AIPS, using the PRTAB task accessing the system temperature extension file, TY. The values labeled “Tant” were interpreted as being the raw system temperature values. Figure 1 shows the raw system temperature data from the 14 EVLA antennas with useable data for the Vertical Scan, IF 1, polarization R. The plots for the other polarization-IF combinations were similar, as well as the data from the other two scans. The horizontal scan had a few low system temperatures at the beginning of the scan, possibly indicating a compression of the system temperature values for these measurements very close to the sun, or that the antennas had not yet reached their first position at $2R_{\odot}$ ($32'$) from the sun. In the next pointing of the Horizontal Scan, and the first 3 pointings of the Diagonal and Vertical Scans, a few of the antennas had relatively high system temperatures, some between 1000-3500 K. The main features of the raw T_{sys} measurements are that from $2-3R_{\odot}$ ($32-48'$) the system temperature ranges from about 100-350 K, from $3-5R_{\odot}$ ($48-80'$) the T_{sys} ranges from about 50-100 K, and from $5-8.9R_{\odot}$ ($80-142'$) the T_{sys} levels off to about 40 K. The constant system temperature past $8R_{\odot}$ ($128'$) seems to indicate that at this distance there is no solar contribution to the system temperature.

Near $9R_{\odot}$ ($143'$) the raw system temperatures for the various antennas range from about 20-50 K. This is interpreted as errors in the calibration of the system temperature, attributable to inaccurate values of the noise diode. This is of no consequence for normal interferometric observations, since most observers' calibration procedures absorb the errors into calibration constants. To average over this calibration error, we normalized the system temperatures to the median values at $8.9R_{\odot}$ ($142'$), and calculated a normalized temperature $T'(r)$ for each antenna, IF, and polarization, given by

$$T'(r) = T(r) \left[\frac{T_{median}}{T(r = 8.9R_{\odot})} \right] \quad (2)$$

where $T(r)$ is the raw system temperature, $T(r = 8.9R_{\odot})$ is the raw system temperature at the greatest angular separation for that antenna, polarization, and IF, and T_{median} is the median value of $T(r = 8.9R_{\odot})$ for all 14 antennas with the same IF and polarization. The ratio $\left[\frac{T_{median}}{T(r = 8.9R_{\odot})} \right]$ serves as a multiplicative normalization constant for each antenna,

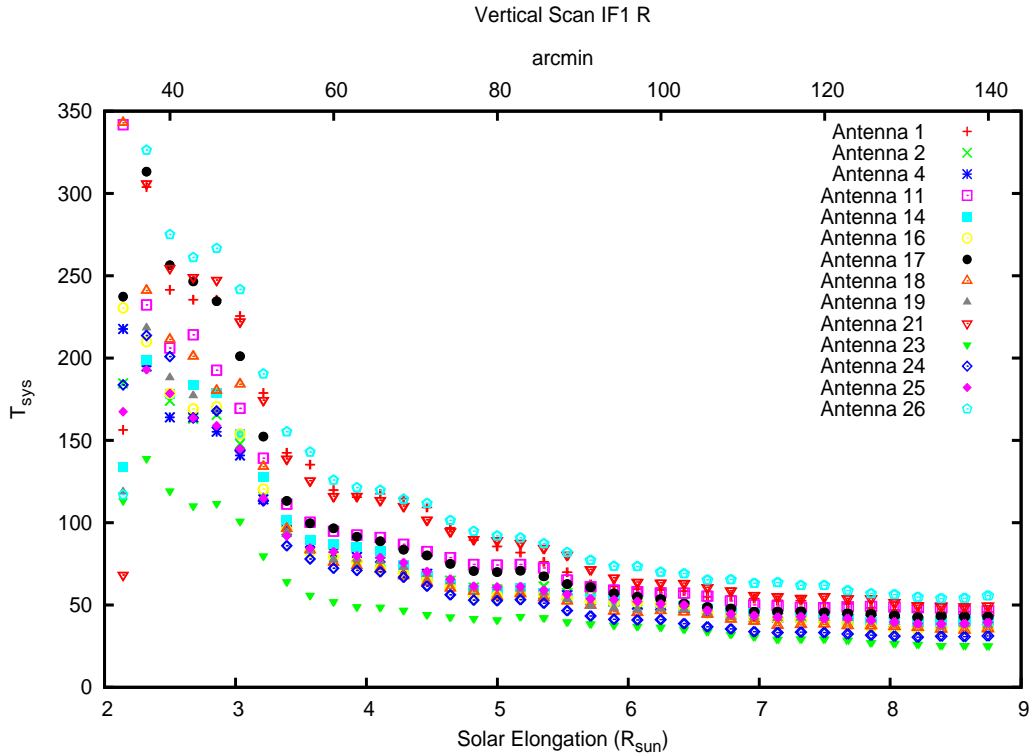


FIG. 1: Unmodified system temperature data for 14 EVLA antennas

IF, and polarization. The normalized system temperatures as a function of r are shown in Figure 2. Figure 2 shows that, after normalizing the data, there was still significant spread in the system temperature values between antennas. At $2R_{\odot}$ ($32'$) the normalized system temperatures range from 100-350 K. The reason for these inter-antenna differences is not entirely clear. Four antennas were eliminated from the data set at this point because they were at wide variance with the remaining antennas.

We wished to condense the data shown in Figure 2 by taking a median of the normalized T_{sys} data. For most of the scans, a few of the antennas had significantly higher system temperatures than the others, as mentioned above, so we found it better to take a median of the data as opposed to a mean, since a median is less affected by outlying points. For each IF at a given solar elongation, T_{sys} measurements for all 10 antennas and both polarizations were included in the distributions from which we calculated the median and range. Instead of the standard deviation as a measure of the range, we chose the upper and lower limits which contained 80% of the measurements at a given pointing. The final result of this

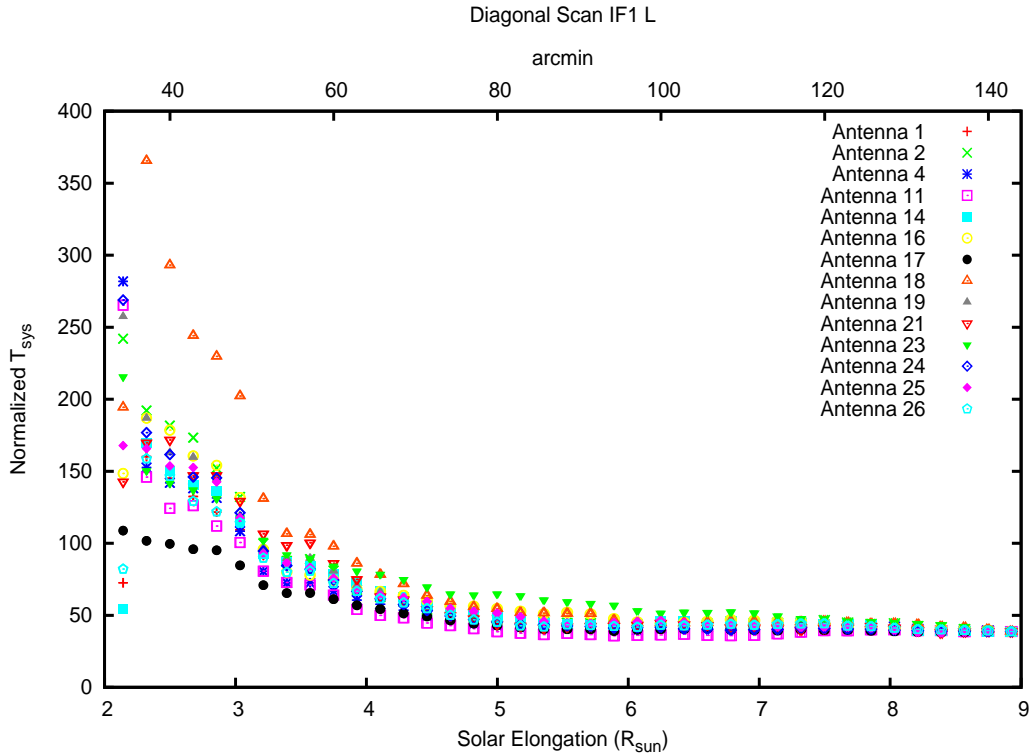


FIG. 2: Normalized system temperature data calculated from equation (1)

process was six empirical functions for $\bar{T}'(r)$, corresponding to the 2 IFs for each of the 3 scans, where $\bar{T}'(r)$ is the median of the $T'(r)$ values. As an example, in Figure 3 we show $\bar{T}'(r)$ corresponding to IF 2 on the diagonal scan.

B. Comparison with Model Curves

The system temperature is a sum of the receiver temperature and the antenna temperature. The receiver temperature should be constant, but the antenna temperature changes when observing near the sun. The expected antenna temperature is proportional to the convolution of the beam power pattern with the brightness temperature distribution of the source. To understand our measurements shown in Figure 3, we calculated an a-priori estimate of the sun-induced antenna temperature as a function of angular offset. To this we added a receiver temperature value of 39 K to obtain a model function $T(r)$. We used a uniform brightness temperature distribution from a VLA 4.6 GHz image of the quiet sun (Stephen White, Univ. of Maryland, private communication), with a brightness temperature

of 15000K (Zirin et al 1991). For the beam power pattern we used Figure 5 from Perley and Hayward (2005), which plots the normalized beam power pattern for several slices through the 4850 MHz beam pattern of EVLA antenna 13. The solar radius used in the model calculation was $16'.25$, which is defined as the radius above a brightness temperature of 10000 K at 4.6 GHz for April 26. A detailed discussion of this calculation is given in Whiting (2009).

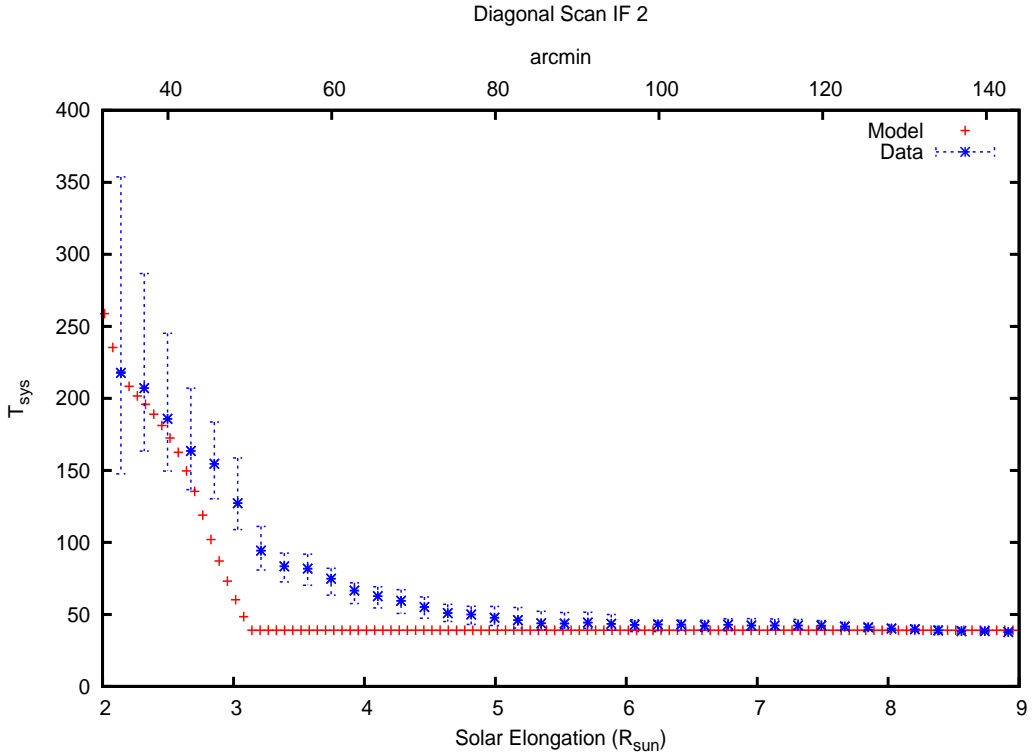


FIG. 3: $\bar{T}'(r)$ for IF2 on the diagonal scan. The “error” bars represent the range which includes 80% of the antennas. The red crosses are system temperature expectations based on a model using the antenna beam pattern in Perley and Hayward (2005).

Figure 3 shows the model $T(r)$ values plotted with the measured $\bar{T}'(r)$ values. The curve reproduces the data at $2-2.5R_{\odot}$ ($32-40'$) and does a very good job of reproducing the system temperature increase near $2R_{\odot}$ ($32'$). However, it subsequently falls off too fast to the receiver temperature value. The reason for this is that the beam power pattern of Perley and Hayward (2005) was only measured out to about $3R_{\odot}$ ($48'$), including only the first and second side lobes. The model curve does not include contributions to the antenna temperature from the antenna response beyond the second sidelobe. The obvious conclusion

to be drawn from Figure 3 is that higher order sidelobes determine the solar contribution to the antenna temperature for $r \geq 3R_{\odot}$ ($48'$).

We estimated the role of additional sidelobes on the antenna temperature as follows. We created a plausible extrapolation of the beam power pattern based on the theoretical expression for a uniformly-illuminated circular aperture (Rohlfs and Wilson 2000),

$$P(r) = \left[\frac{2J_1(\pi r D/\lambda)}{\pi r D/\lambda} \right]^2 \quad (3)$$

where $J_1(x)$ is a Bessel Function of the first kind. We noticed that the first and second sidelobes of the measured power pattern were twice as high as predicted by equation (3). Our estimate of the third sidelobe included this effect. We recalculated the model $T(r)$ with an extrapolated third sidelobe appended to the beam pattern of Perley and Hayward (2005). This third sidelobe had 0.3% of the forward gain (-25 dB) and peaked at $3.4R_{\odot}$ ($55'$) from the beam center. Calculation of a model $T(r)$ with a beam possessing the extrapolated and extended third sidelobe tended to overestimate the system temperature in comparison with the data. By a process of trial and error we determined a third sidelobe level which appeared to provide a good match to the measured data. The location of this third sidelobe was kept at the offset from the beam center indicated by equation (3). A comparison of a model $T(r)$, including a third sidelobe level of 0.2% (-27 dB) of the forward gain is shown in Figure 4.

The addition of the extrapolated third sidelobe matches the data at separations greater than about $2.5R_{\odot}$ ($40'$). Between $2-2.5R_{\odot}$ ($32-40'$) the model slightly overestimates the median system temperature, yet it is well within the range of the data. Figure 4 indicates that a third sidelobe is needed in the model to reproduce the measured data. The underestimate of the system temperature in the model near $5R_{\odot}$ ($80'$) seems to indicate that side lobes of order higher than three may also be contributing to the system temperatures, although at a very low level.

Our main result is that the measured beam pattern, supplemented by a plausible though unmeasured third sidelobe, together with an independent representation of the brightness distribution of the quiet sun, provides a good representation of the measured 5 GHz system temperature of the EVLA. Figure 4 may be used in planning, and determining the sensitivity for, future EVLA observations at 5 GHz.

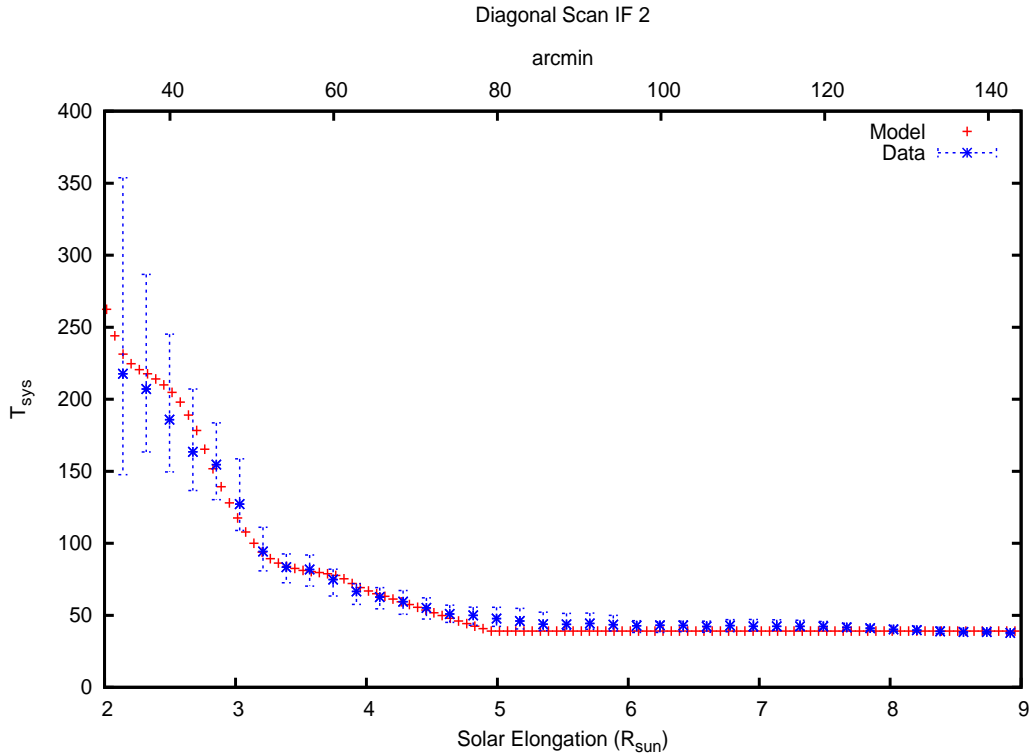


FIG. 4: Red points represent the theoretical model using a plausible extrapolation of the antenna beam pattern past $3R_{\odot}$ ($48'$).

IV. SUMMARY

The results of this investigation are summarized below.

1. EVLA test measurements were taken on April 26, 2009 to measure the solar contribution to the system temperature at 5 GHz as a function of angular distance from the sun.
2. The EVLA antennas need calibration due to the observed spread of cold-sky system temperature values. Normally, this should not be a concern, since most calibration procedures account for this.
3. After normalization, the system temperatures still showed significant antenna-to-antenna variance, especially at $2-3R_{\odot}$ ($32-48'$). The reason for this is unknown.
4. The C-band system temperatures at a pointing offset of 8 solar radii ($128'$) and greater

do not appear to show any T_{sys} enhancement due to the sun. From $3-5R_{\odot}$ (48-80') the median system temperatures range from 50-100 K and between $2-3R_{\odot}$ (32-48') they range from 100-350 K.

5. A theoretical model using an extrapolated antenna beam pattern can adequately represent the T_{sys} values as a function of solar offset.
6. A final point is that these measurements were made during the anomalously low solar minimum between solar cycles 23 and 24. It is probable that a future observer could experience higher system temperatures than those reported here, due to the presence of active regions on the sun.

Acknowledgments

This work was supported at the University of Iowa by grant ATM03-54782 from the National Science Foundation, Division of Atmospheric Sciences.

-
- [1] L.D. Ingleby, S.R. Spangler and C.A. Whiting, ApJ **370**, 779 (2007).
 - [2] R. Perley and B. Hayward, EVLA Memo **90**, (2005).
 - [3] K. Rohlfs and T.L. Wilson, Tools of Radio Astronomy, Springer-Verlag, (2000).
 - [4] C.A. Whiting, M.S. Thesis, University of Iowa, (In preparation; 2009).
 - [5] H. Zirin, B.M. Baumert and G.J. Hurford, ApJ **668**, 520 (1991).